Strongly Bound Dibaryon with Maximal Beauty Flavor from Lattice QCD

Nilmani Mathur,[1,*] M. Padmanath,[2,†,§] and Debsubhra Chakraborty[1,‡]
[1]*Department of Theoretical Physics, Tata Institute of Fundamental Research, Homi Bhabha Road, Mumbai 400005, India*
[2]*Helmholtz Institut Mainz, Staudingerweg 18, 55128 Mainz, Germany and GSI Helmholtzzentrum für Schwerionenforschung GmbH, Planckstr. 1, 64291 Darmstadt, Germany*

(Received 25 May 2022; revised 9 January 2023; accepted 16 February 2023; published 16 March 2023)

We report the first lattice QCD study of the heavy dibaryons in which all six quarks have the bottom (beauty) flavor. Performing a state-of-the-art lattice QCD calculation we find clear evidence for a deeply bound Ω_{bbb}-Ω_{bbb} dibaryon in the $^1S_0$ channel, as a pole singularity in the S-wave Ω_{bbb}-Ω_{bbb} scattering amplitude with a binding energy $-81(^{+14}_{-16})$ MeV. With such a deep binding, Coulomb repulsion serves only as a perturbation on the ground state wave function of the parametrized strong potential and may shift the strong binding only by a few percent. Considering the scalar channel to be the most bound for single flavored dibaryons, we conclude this state is the heaviest possible most deeply bound dibaryon in the visible universe.

DOI: 10.1103/PhysRevLett.130.111901

Understanding baryon-baryon interactions from first principles is of prime interest in nuclear physics, cosmology, and astrophysics [1–4]. Dibaryons are the simplest nuclei with baryon number 2, in which such interactions can be studied transparently. However, the only known stable dibaryon is deuteron and the possible observation of perhaps just one more unstable light dibaryon [$d^*(2380)$] has recently been reported [5,6]. Even so, based on the theory of strong interactions, one expects to have more dibaryons in nature, particularly with the strange and heavy quark contents. *Ab initio* theoretical investigations using lattice QCD are well suited for studying such hadrons and indeed it can play a major role in their future discovery.

Lattice QCD calculations of dibaryon systems are becoming more feasible now particularly in the light and strange quark sectors [7–21]. Even so, such studies involving heavy flavors are limited to only a few calculations [22–25]. Among the heavy dibaryons, a system of two Ω_{QQQ} baryons ($Q \equiv c$, b) provides a unique opportunity to investigate baryon-baryon interactions and associated nonperturbative features of QCD in a chiral dynamics free environment. Such a system in the strange sector have been studied using Lüscher's finite-volume formalism [26], which suggested that the Ω-Ω channel is weakly repulsive [10]. Another study using the HALQCD procedure [27] suggested that the system is not attractive enough to form a bound state [12]. A recent high statistics HALQCD study [14] on a very large volume (~8 fm) claimed that such a system is weakly attractive and the strength of potential is enough to form a very shallow bound state. Although the inferences from different procedures differ, they all agree on the fact that the interaction between two Ω baryons is weak. Another recent HALQCD investigation of Ω_{ccc}-Ω_{ccc} dibaryon reported a shallow bound state in the $^1S_0$ channel [24]. While all these investigations suggest that the interactions in two Ω_{QQQ} baryon systems are rather weak with quark masses ranging from light to charm, several lattice studies in the recent years on heavy dibaryons [23,25] and heavy tetraquarks [28–31] have shown that multihadron systems with multiple bottom quarks can have deep binding. Hence, it is very timely to study Ω_{bbb}-Ω_{bbb} interactions using lattice QCD. Note that very little is known about it through other theoretical approaches [32–34].

The motivation for such a study is multifold. Theoretically it can provide an understanding of the strong dynamics of multiple heavy quarks in a hadron. In cohort with results from single- [10,12,24,35], double- [11,15,18–21,23,25,36–38], and triple-flavored dibaryons [7–9,11,13,16–18,39], particularly those with heavier quarks, one would be able to build a broader picture of the baryon-baryon interactions at multiple scales. This can illuminate the physics of heavy quark dynamics in nonmesonic hadrons. A study of the quark-mass dependence of scattering parameters can further shed light into the dominant dynamics in different regimes. Indication of possible promising channels on any bound heavy dibaryon from such studies can also stimulate future experimental searches for them, as in the case of heavier tetraquarks [40–43].

In this Letter, we report the first lattice QCD investigation of the ground state of the dibaryons with the highest number of bottom (beauty) quarks in the $^1S_0$ channel. We name it $\mathcal{D}_{6b} \equiv \Omega_{bbb}$-$\Omega_{bbb}$, a dibaryon formed out of a combination of two Ω_{bbb} baryons. Using various state-of-the-art lattice QCD utilities and methodologies, we extract the mass of $\mathcal{D}_{6b}$ and find clear evidence for a strongly bound state, with a binding energy of $-81(^{+14}_{-16})(14)$ MeV, and a scattering length of $0.18(^{+0.02}_{-0.02})(0.02)$ fm. Despite its compactness, we find the Coulomb interactions act only as a perturbation to the strong interactions and do not change the binding in any significant way. Upon comparison to the binding energies of other dibaryons, e.g., 2.2 MeV of deuteron, and other strange or heavy dibaryons [23,24], we conclude $\mathcal{D}_{6b}$ to be the most deeply bound heaviest possible dibaryon in our visible universe.

The lattice setup that we use here is similar to the one used in Refs. [30,44] and we discuss it below.

Lattice ensembles.—We employ four lattice QCD ensembles with dynamical u/d, s, and c quark fields, generated by the MILC Collaboration [45] with highly improved staggered quark (HISQ) fermion action [46], as shown in Fig. 1. Lattice spacings are determined using r_1 parameter [45], which are found to be consistent with the scales obtained through Wilson flow [47].

Bottom quarks on lattice.—Since the bottom quark is very heavy, we use a nonrelativistic QCD (NRQCD) Hamiltonian [48], including improvement coefficients up to $\mathcal{O}(\alpha_s v^4)$ [49]. Quark propagators are calculated from the evolution of NRQCD Hamiltonian with Coulomb gauge fixed wall sources at multiple source time slices. We tune the bottom quark mass using the Fermilab prescription for heavy quarks [50] in which we equate the lattice-extracted spin-averaged kinetic mass of the $1S$ bottomonia states with its physical value [51]. Such a tuning was also used in Refs. [23,30,44] and was found to reproduce the physical value of the hyperfine splitting of $1S$ bottomonia.

(Di)baryon interpolators.—For the single Ω_{bbb} baryon, we use the quasilocal nonrelativistic operator with $J^P = 3/2^+$, as was used in Ref. [10]. This operator was constructed by the LHPC Collaboration and is listed in Table VII of Ref. [52] and also detailed in Ref. [53]. For extracting the ground state mass we assume only S-wave

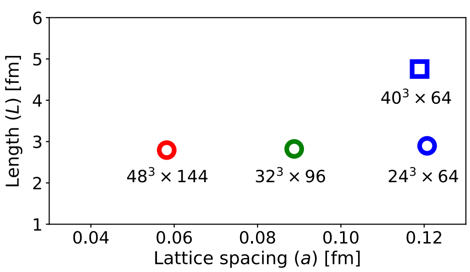

FIG. 1. Lattice QCD ensembles, with sizes $N_s^3 \times N_t$, used in this work. Here, $L = N_s a$ is the spatial extent of the lattice.

interactions in two baryon systems where the overall state is antisymmetric under the exchange of two baryons. Denoting components of the $J = 3/2$ Ω_{bbb} operator ($\mathcal{O}_{\Omega_{bbb}}$) with χ_m, m being the azimuthal component of J, we construct the Ω_{bbb}-Ω_{bbb} dibaryon operators as

$$\mathcal{O}_{\mathcal{D}_{6b}}(x,t) = \chi_m(x,t)[CG]^{mn}\chi_n(x,t). \quad (1)$$

Here, $[CG]^{mn}$ are the relevant spin-projection matrix constructed out of the appropriate Clebsch-Gordon coefficients. The $J = 0$ dibaryon operator that we employ in this work is given by [10,53]

$$\mathcal{O}_{\mathcal{D}_{6b}^{J=0}} = \frac{1}{2}[\chi_{\frac{3}{2}}\chi_{-\frac{3}{2}} + \chi_{-\frac{1}{2}}\chi_{\frac{1}{2}} - \chi_{\frac{1}{2}}\chi_{-\frac{1}{2}} - \chi_{-\frac{3}{2}}\chi_{\frac{3}{2}}]. \quad (2)$$

Using these baryon and dibaryon operators ($\mathcal{O}_{\Omega_{bbb}}$ and $\mathcal{O}_{\mathcal{D}_{6b}}$) we compute two-point correlation functions between the source (t_i) and sink (t_f) time slices,

$$C_{\mathcal{O}}(t_f - t_i) = \sum_{\vec{x}_f} e^{-i\vec{p}.\vec{x}_f}\langle 0|\mathcal{O}(\vec{x}_f, t_f)\bar{\mathcal{O}}(t_i)|0\rangle. \quad (3)$$

At the sink time slice, we use several different quark field smearing procedures to identify the reliable ground state plateau and quantify possible excited state contamination (see Ref. [53] for more details). Ground state masses for the single and the dibaryon are obtained by fitting the respective average correlation function with a single exponential at large times ($\tau = t_f - t_i$).

While determining mass in a lattice calculation it is often useful to plot the effective mass, defined as $m_{eff}a = \log[\langle C(\tau)\rangle/\langle C(\tau+1)\rangle]$, to show the signal saturation and justify the time window to be chosen in the exponential fit. In Fig. 2, we present the effective masses for $C^2_{\Omega_{bbb}}$ (green circles) and $C_{\mathcal{D}_{6b}}$ (blue squares) on the finest ensemble ($a \sim 0.06$ fm) using wall quark sources and point quark sinks. We make the following observations from this result: (i) The signal in the effective masses

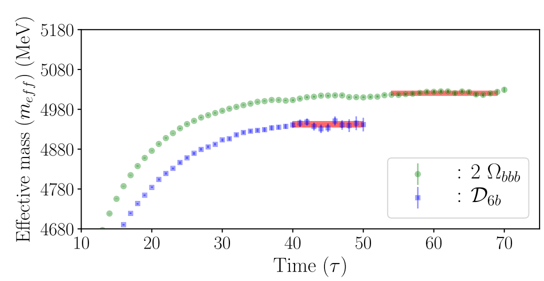

FIG. 2. Effective masses corresponding to the ground states of the noninteracting two-baryon and dibaryon correlators on the finest lattice ensemble determined from wall-to-point correlation functions. An energy gap between them is clearly visible at all time slices. The solid bands show the fit estimates and fit windows.

saturates well before the noise takes over, and hence one can reliably extract the respective ground state masses. (ii) The signal in the noninteracting $2\Omega_{bbb}$ level survives until large times. This is because $2\Omega_{bbb}$ level is obtained from the single baryon Ω_{bbb} correlator that decays with an exponent of $M_{\Omega_{bbb}} < M_{\mathcal{D}_{6b}}$, and hence can propagate further than the $\mathcal{D}_{6b}$ state. (iii) Most importantly, it is quite evident that there is a clear energy gap between the ground state energy levels of the noninteracting two-baryon and the dibaryon systems at all times. This clearly shows that the ground state mass of dibaryon $M_{\mathcal{D}_{6b}}$ is smaller than that of the noninteracting level $2M_{\Omega_{bbb}}$. We find similar energy differences for all the ensembles and we discuss the results below. Based on the $t_{\rm min}$ dependence of the fits, which are discussed in Ref. [53], we make our final choices for the fit ranges and uncertainties arising out of such choices.

In order to gauge the extent of excited state contaminations in our estimates, we carry out two additional calculations: one with a wall source and a Gaussian-smeared sink [64,65], and the other with a wall source and spherical-box sink [66]. The results are detailed in the Supplemental Material [53]. We find that results are clearly consistent between different measurement setups and validate our estimates. We pass the results from all these different smearing procedures through the scattering analysis, as discussed below, to determine uncertainties related to the excited state contamination. Moreover, an effective mass analysis using Prony's method [67–69] and a lattice setup with displaced baryons [53], further reinforce the findings of two clearly separated energy levels as in Fig. 2 [53].

Next, we calculate the energy difference between the ground state of the dibaryon ($\mathcal{D}_{6b}$) and the noninteracting two baryons ($2\,\Omega_{bbb}$):

$$\Delta E = M_{\mathcal{D}_{6b}} - 2M_{\Omega_{bbb}}. \quad (4)$$

In Table I, we present ΔE for all the lattice ensembles. We quote the average of various fitting and smearing procedures as the central value of energy splittings in separate ensembles. The largest deviation in these energy splittings extracted from different procedures is taken as the systematics related to the excited state effects. We find ΔE to be always *negative* and several standard deviations (σ) away from zero. This observation on multiple ensembles, with three different lattice spacings, two different volumes, and different energy extraction procedures leads us to unambiguously conclude that there is an energy level below the threshold.

TABLE I. Energy difference $\Delta E = M_{\mathcal{D}_{6b}} - 2M_{\Omega_{bbb}}$ in MeV on different ensembles.

Ensemble	ΔE	Ensemble	ΔE
$24^3 \times 64$	−61(11)	$40^3 \times 64$	−62(7)
$32^3 \times 96$	−68(9)	$48^3 \times 144$	−71(7)

Scattering analysis.—To establish the existence of a state from these energy levels in terms of pole singularities in the $\Omega_{bbb}\Omega_{bbb}$ S-wave scattering amplitudes across the complex Mandelstam s plane, we use the generalized form of finite-volume formalism proposed by M. Lüscher [26]. For the scattering of two spin-3/2 particles in the S wave leading to a total angular momentum and parity $J^P = 0^+$, the phase shifts $\delta_0(k)$ are related to the finite-volume energy spectrum via Lüscher's relation:

$$k\,\cot[\delta_0(k)] = \frac{2Z_{00}[1; (\frac{kL}{2\pi})^2]}{L\sqrt{\pi}}. \quad (5)$$

Here, k is the momentum of Ω_{bbb} in the center of momentum frame and is given by

$$k^2 = \frac{\Delta E}{4}(\Delta E + 4M^{\rm phys}_{\Omega_{bbb}}), \quad (6)$$

where ΔE is the energy differences listed in Table I, and $M^{\rm phys}_{\Omega_{bbb}}$ is the mass of Ω_{bbb} in the continuum limit. The S-wave scattering amplitude is given by $t = (\cot\delta_0 - i)^{-1}$, and a pole in t related to a bound state happens when $k\,\cot\delta_0 = -\sqrt{-k^2}$. We parametrize $k\,\cot\delta_0 = -1/a_0$, where a_0 is the scattering length. The scattering analysis is performed following the procedure outlined in Appendix B of Ref. [70], such that the best fit parameters are constrained to satisfy Eq. (5). To estimate the systematic uncertainties from the lattice cutoff effects, we perform several different fits involving different subsets of the four levels with $k\,\cot\delta_0$ parametrized either as a constant or as a constant plus a linear term in the lattice spacing. All of the fits indicate the existence of a deeply bound state. We find that the best fit corresponds to the one that considers all energy levels and incorporates the lattice spacing a dependence of the scattering length with a linear parametrization $k\,\cot\delta_0 = -1/a_0^{[0]} - a/a_0^{[1]}$. We present this as our main result, leading to a $\chi^2/{\rm d.o.f} = 0.7/2$, with the following best fit parameters and binding energy:

$$a_0^{[0]} = 0.18(^{+0.02}_{-0.02})\ {\rm fm}, \qquad a_0^{[1]} = -0.18(^{+0.18}_{-0.11})\ {\rm fm}^2, \quad (7)$$

$$\text{and} \quad \Delta E_{\mathcal{D}_{6b}} = -81(^{+14}_{-16})\ {\rm MeV}. \quad (8)$$

In Fig. 3, we present details of our main results. On the top pane, the analytically reconstructed finite-volume energy levels (black stars) from best fit parameters in Eq. (7) can be seen to be in agreement with the simulated energy levels (large symbols), indicating quality of fit. In the middle pane, we plot $k\,\cot\delta_0$ versus k^2 in units of the energy of the threshold. The orange dashed curve is the bound state constraint $\sqrt{-k^2}$ and the red solid line is the fitted $k\,\cot\delta_0$

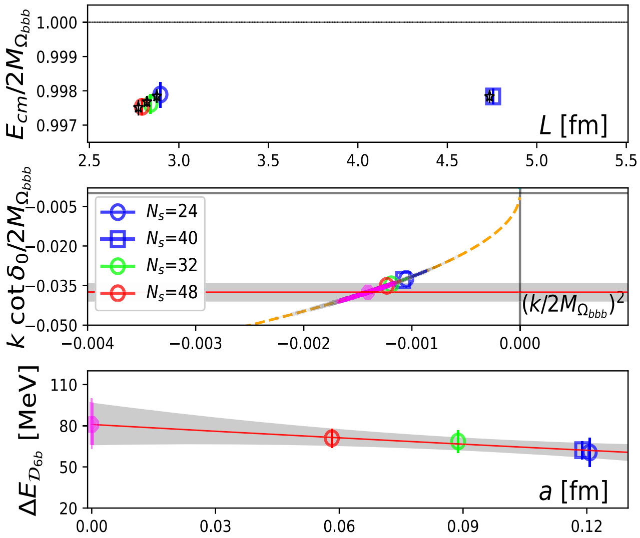

FIG. 3. Results from the finite-volume scattering analysis. Top: Comparison of the simulated energy levels (large symbols) with the energy levels (black stars) analytically reconstructed using Eq. (7), indicating the quality of the scattering analysis fit. Middle: $k \cot \delta_0$ versus k^2 in units of energy of the threshold ($2M_{\Omega_{bbb}}$) and information on poles in t indicated by magenta symbols. Bottom: Continuum extrapolation of the binding energy in Eq. (8) determined from fitted scattering amplitude in Eq. (7).

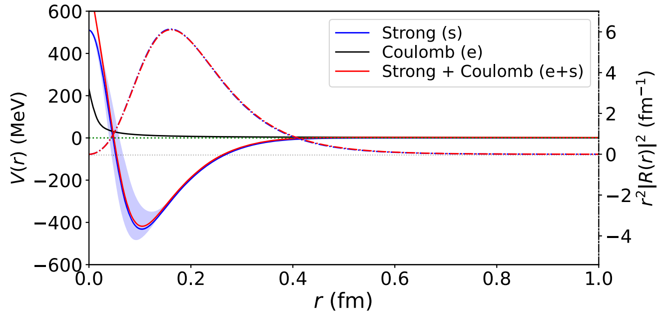

FIG. 4. Coulomb (V_e), the parametrized strong potentials (V_s) and their sum are shown by the black, blue, and red curves, respectively. The shaded region represents the variation of V_s with respect to its parameters. V_e is evaluated at a rms charge radius equal to the rms radius of the V_s ground state. The radial probability densities of the ground state wave functions of the strong and combined potentials are shown by the dashed-dotted curves.

in the continuum limit. The crossing between these two curves, highlighted by the magenta symbol, is the bound state pole position in t. In the bottom pane, we present the continuum extrapolation of binding energy leading to the value in Eq. (8) compared with the simulated energy levels at the respective lattice spacings. The magenta symbol represents the binding energy in the continuum limit, with thick error representing the statistical and fit window error. The thin error includes the systematics related to excited state effects added in quadrature.

Coulomb repulsion.—With two units of electric charge in the system, the effect of Coulomb repulsion on the binding energy of this dibaryon could be important. To gauge that, we perform an analysis, as in Ref. [24], and detail that in the Supplemental Material [53]. We model the strong interactions between two interacting Ω^-_{bbb} baryons with a quantum mechanical multi-Gaussian attractive potential, constrained to match the binding energy $-81(^{+14}_{-16})$ MeV that we find in this Letter. In Fig. 4, we present the model potentials for strong and Coulombic interactions and also their combination, together with the radial probabilities of the ground state wave functions in the strong and combined potentials. Evidently, the Coulombic potential hardly affects the strong interaction potential in the length scales where the ground state probabilities peak and infer that it serves only as a perturbation. The associated maximum change in binding energy is found to be between 5 and 10 MeV.

After addressing the systematic errors along with excited state contaminations [53] the final value of the dibaryon mass is determined by adding $\Delta E_{\mathcal{D}_{6b}}$ $[-81(^{+14}_{-16})(14)$ MeV$]$ with the two-baryon mass $2M_{\Omega_{bbb}}$. Since the Ω_{bbb} baryon mass is unknown we use its lattice extracted value. To this end, we perform continuum extrapolation of the energy splitting $M_{\Omega_{bbb}}(a) - \frac{3}{2}M_{\overline{1S}}(a)$, and then add $3/2M^{\rm phys}_{\overline{1S}}$, with $M^{\rm phys}_{\overline{1S}} =$ 9445 MeV [71], to that. Thus, we arrive at $M^{\rm phys}_{\Omega_{bbb}} =$ 14366(7)(9) MeV, which is consistent with other lattice results [72]. Using that, we obtain $M^{\rm phys}_{\mathcal{D}_{6b}} = 2M^{\rm phys}_{\Omega_{bbb}} + \Delta E_{\mathcal{D}_{6b}} = 28651(^{+16}_{-17})(15)$ MeV. Possible effects of Coulomb repulsion are included in the systematic errors.

Error budget.—Finally we address the possible sources of errors in this calculation. We use a lattice setup with $2+1+1$ flavored HISQ fermions where the gauge fields are Symanzik-improved at $\mathcal{O}(\alpha_s a^2)$, and the NRQCD Hamiltonian has improvement coefficients up to $\mathcal{O}(\alpha_s v^4)$. Such a lattice setup has shown to reproduce energy splittings in bottomonia with a uncertainty of about 6 MeV [53]. Note that here we are calculating the energy difference in which some of the systematics get reduced. For the dibaryon ground state in the finite volume, statistical, excited-state-contamination, and fit-window errors are the main sources of error. The energy levels are extracted using single exponential fits to the correlation functions from rigorously identified ground state plateau regions [53]. Correlated averages of various fitting intervals are considered to arrive at conservative fitting-window errors. Statistical and fit window errors are added in quadrature, and then convolved through the Lüscher's analysis and continuum extrapolation. The excited state contamination is determined from differences in the continuum limit estimates from the scattering analysis using results from different sink smearing procedures followed. However, it still would be worthwhile to investigate excited state uncertainties more precisely in future variational calculations. Other possible sources of errors are related to the continuum extrapolation fit forms, scale setting, quark mass tuning, and electromagnetic corrections that together are found to be 12 MeV in such energy splittings, as detailed in the Supplemental Material [53]. Various errors are finally added in quadrature, yielding a total error of about 20% for the binding energy. Our results and inferences are robust up to the statistical and systematic uncertainties we have determined.

Summary and outlook.—In this Letter, using lattice QCD we present a first investigation of the dibaryons in which all six quarks have bottom flavor and find a deeply bound dibaryon ($\mathcal{D}_{6b} \equiv \Omega_{bbb} - \Omega_{bbb}$) in the ${}^1S_0$ channel. Following Lüscher's formalism, we determine the relevant scattering amplitude, and after considering possible systematic uncertainties [53], we identify a bound state pole with a binding energy $-81(^{+14}_{-16})(14)$ MeV relative to the threshold $2M_{\Omega_{bbb}}$. The mass of $\mathcal{D}_{6b}$ dibaryon corresponding to this pole is found to be $28\,651(^{+16}_{-17})(15)$ MeV. Although this dibaryon is expected to be compact, we find the Coulomb repulsion within this dibaryon acts only as a perturbation to the strong interactions and may shift the mass only by a few percent. The use of complementary measurements and analysis procedures in identifying the real ground state plateau ensure the robustness of our results. Our results provide intriguing evidence for the existence of the bound $\mathcal{D}_{6b}$ state, and it would surely motivate both phenomenological studies of its detection as well as follow-up lattice QCD studies investigating hard-to-quantify excited-state uncertainties more precisely.

It is interesting to observe that the interactions between similar baryons using different procedures at the strange and charm quark masses are found to be very weak [10,12,14,24]. Note that a clear consensus on such systems with possible near threshold features requires complementary investigations of the same system with same high statistics ensembles but with different procedures. In comparison with the light and strange sectors, the binding energy of multiquark hadrons involving more than one bottom quark are predicted to be large [23,28–31,73,74]. In this Letter, we also observe the similar pattern in the $\Omega_{bbb}\Omega_{bbb}$ channel. Taken together a common interesting pattern is emerging that the presence of more than one bottom quark enhances the binding in multihadron systems, which needs to be understood thoroughly including the quark mass dependence of scattering parameters.

Although a direct identification of $\mathcal{D}_{6b}$ dibaryon is a long way off, our results on this heavy dibaryon, particularly because of its deep binding, will provide a major impetus in experimental searches for heavy quark exotics. Very much like the discovery of Ξ_{cc} leading to predictions of various possible heavy multiquark systems [73], the discovery of doubly bottom baryons would be an important step in filling up the blanks higher up in the hadronic reaction cascade bringing prospects for discovering various bottom quark exotics, including $\mathcal{D}_{6b}$. Given the recent excitements in the search for new heavy exotics [75–77] with multiple theoretical proposals and ideas [40–43], it is highly anticipated that substantial efforts, both on the theoretical as well as experimental fronts, would be steered and accelerated in this direction in the coming years.

This work is supported by the Department of Atomic Energy, Government of India, under Project Identification No. RTI 4002. We are thankful to the MILC Collaboration and in particular to S. Gottlieb for providing us with the HISQ lattice ensembles. We thank D. Mohler for a careful reading of the manuscript. We thank the authors of Ref. [78] for making the "TwoHadronsInBox" package used in this work and in particular Colin Morningstar for his help with the package. We also thank T. Doi, L. Liu, T. Luu, M. Pappagallo, and S. Paul for discussions. Computations are carried out on the Cray-XC30 of ILGTI, TIFR. N. M. would also like to thank A. Salve, K. Ghadiali, and P. M. Kulkarni for computational supports.

[*]Corresponding author.
nilmani@theory.tifr.res.in
[†]Corresponding author.
padmanath@imsc.res.in
[‡]Corresponding author.
debsubhra.chakraborty@tifr.res.in
[§]Present address: The Institute of Mathematical Sciences, HBNI, Taramani, Chennai 600113, India.

[1] R. V. Wagoner, W. A. Fowler, and F. Hoyle, On the synthesis of elements at very high temperatures, Astrophys. J. **148**, 3 (1967).
[2] D. N. Schramm and M. S. Turner, Big-bang nucleosynthesis enters the precision era, Rev. Mod. Phys. **70**, 303 (1998).
[3] E. Epelbaum, H.-W. Hammer, and U.-G. Meißner, Modern theory of nuclear forces, Rev. Mod. Phys. **81**, 1773 (2009).
[4] C. Drischler, W. Haxton, K. McElvain, E. Mereghetti, A. Nicholson, P. Vranas, and A. Walker-Loud, Towards grounding nuclear physics in QCD, Prog. Part. Nucl. Phys. **121**, 103888 (2021).
[5] A. P. *et al.* (WASA-at-COSY Collaboration and SAID Data Analysis Center), Evidence for a New Resonance from Polarized Neutron-Proton Scattering, Phys. Rev. Lett. **112**, 202301 (2014).
[6] R. Molina, N. Ikeno, and E. Oset, Sequential single pion production explaning the dibaryon "$d^*(2380)$" peak, arXiv:2102.05575.
[7] S. R. Beane, E. Chang, W. Detmold, B. Joo, H. W. Lin, T. C. Luu, K. Orginos, A. Parreño, M. J. Savage, A. Torok, and A. Walker-Loud (NPLQCD Collaboration), Evidence for a Bound *H* Dibaryon from Lattice QCD, Phys. Rev. Lett. **106**, 162001 (2011).
[8] T. Inoue, N. Ishii, S. Aoki, T. Doi, T. Hatsuda, Y. Ikeda, K. Murano, H. Nemura, and K. Sasaki (HAL QCD Collaboration), Bound *H* Dibaryon in Flavor SU(3) Limit of Lattice QCD, Phys. Rev. Lett. **106**, 162002 (2011).
[9] Z.-H. Luo, M. Loan, and Y. Liu, Search for *H* dibaryon on the lattice, Phys. Rev. D **84**, 034502 (2011).
[10] M. I. Buchoff, T. C. Luu, and J. Wasem, *S*-wave scattering of strangeness -3 baryons, Phys. Rev. D **85**, 094511 (2012).

[11] E. Berkowitz, T. Kurth, A. Nicholson, B. Joo, E. Rinaldi, M. Strother, P. M. Vranas, and A. Walker-Loud, Two-nucleon higher partial-wave scattering from lattice QCD, Phys. Lett. B **765**, 285 (2017).
[12] M. Yamada, K. Sasaki, S. Aoki, T. Doi, T. Hatsuda, Y. Ikeda, T. Inoue, N. Ishii, K. Murano, and H. Nemura (HAL QCD Collaboration), ΩΩ interaction from $2+1$ flavor lattice QCD, Prog. Theor. Exp. Phys. **2015**, 071B01 (2015).
[13] A. Francis, J. R. Green, P. M. Junnarkar, C. Miao, T. D. Rae, and H. Wittig, Lattice QCD study of the H dibaryon using hexaquark and two-baryon interpolators, Phys. Rev. D **99**, 074505 (2019).
[14] S. Gongyo, K. Sasaki, S. Aoki, T. Doi, T. Hatsuda, Y. Ikeda, T. Inoue, T. Iritani, N. Ishii, T. Miyamoto, and H. Nemura (HAL QCD Collaboration), Most Strange Dibaryon from Lattice QCD, Phys. Rev. Lett. **120**, 212001 (2018).
[15] S. Aoki and T. Doi, Lattice QCD and baryon-baryon interactions: HAL QCD method, Front. Phys. **8**, 307 (2020).
[16] J. R. Green, A. D. Hanlon, P. M. Junnarkar, and H. Wittig, Weakly Bound H Dibaryon from SU(3)-Flavor-Symmetric QCD, Phys. Rev. Lett. **127**, 242003 (2021).
[17] S. Amarasinghe, R. Baghdadi, Z. Davoudi, W. Detmold, M. Illa, A. Parreno, A. V. Pochinsky, P. E. Shanahan, and M. L. Wagman, A variational study of two-nucleon systems with lattice QCD, arXiv:2108.10835.
[18] S. R. Beane, E. Chang, S. D. Cohen, W. Detmold, P. Junnarkar, H. W. Lin, T. C. Luu, K. Orginos, A. Parreño, M. J. Savage, and A. Walker-Loud (NPLQCD Collaboration), Nucleon-nucleon scattering parameters in the limit of SU(3) flavor symmetry, Phys. Rev. C **88**, 024003 (2013).
[19] T. Yamazaki, K.-i. Ishikawa, Y. Kuramashi, and A. Ukawa, Helium nuclei, deuteron, and dineutron in $2+1$ flavor lattice QCD, Phys. Rev. D **86**, 074514 (2012).
[20] M. L. Wagman, F. Winter, E. Chang, Z. Davoudi, W. Detmold, K. Orginos, M. J. Savage, and P. E. Shanahan, Baryon-baryon interactions and spin-flavor symmetry from lattice quantum chromodynamics, Phys. Rev. D **96**, 114510 (2017).
[21] B. Hörz *et al.*, Two-nucleon S-wave interactions at the $SU(3)$ flavor-symmetric point with $m_{ud} \simeq m_s^{\mathrm{phys}}$: A first lattice QCD calculation with the stochastic Laplacian Heaviside method, Phys. Rev. C **103**, 014003 (2021).
[22] T. Miyamoto *et al.*, $\Lambda_c N$ interaction from lattice QCD and its application to Λ_c hypernuclei, Nucl. Phys. **A971**, 113 (2018).
[23] P. Junnarkar and N. Mathur, Deuteronlike Heavy Dibaryons from Lattice Quantum Chromodynamics, Phys. Rev. Lett. **123**, 162003 (2019).
[24] Y. Lyu, H. Tong, T. Sugiura, S. Aoki, T. Doi, T. Hatsuda, J. Meng, and T. Miyamoto, Dibaryon with Highest Charm Number near Unitarity from Lattice QCD, Phys. Rev. Lett. **127**, 072003 (2021).
[25] P. M. Junnarkar and N. Mathur, Study of three-flavored heavy dibaryons using lattice QCD, Phys. Rev. D **106**, 054511 (2022).
[26] M. Luscher, Two particle states on a torus and their relation to the scattering matrix, Nucl. Phys. **B354**, 531 (1991).
[27] N. Ishii, S. Aoki, and T. Hatsuda, The Nuclear Force from Lattice QCD, Phys. Rev. Lett. **99**, 022001 (2007).
[28] P. Bicudo and M. Wagner (European Twisted Mass Collaboration), Lattice QCD signal for a bottom-bottom tetraquark, Phys. Rev. D **87**, 114511 (2013).
[29] A. Francis, R. J. Hudspith, R. Lewis, and K. Maltman, Lattice Prediction for Deeply Bound Doubly Heavy Tetraquarks, Phys. Rev. Lett. **118**, 142001 (2017).
[30] P. Junnarkar, N. Mathur, and M. Padmanath, Study of doubly heavy tetraquarks in Lattice QCD, Phys. Rev. D **99**, 034507 (2019).
[31] L. Leskovec, S. Meinel, M. Pflaumer, and M. Wagner, Lattice QCD investigation of a doubly-bottom $\bar{b}\bar{b}ud$ tetraquark with quantum numbers $i(J^P) = 0(1^+)$, Phys. Rev. D **100**, 014503 (2019).
[32] H. Huang, J. Ping, X. Zhu, and F. Wang, Full heavy dibaryons, Eur. Phys. J. C **82**, 805 (2022).
[33] M.-Z. Liu and L.-S. Geng, Prediction of an ΩbbbΩbbb dibaryon in the extended one-boson exchange model, Chin. Phys. Lett. **38**, 101201 (2021).
[34] J.-M. Richard, A. Valcarce, and J. Vijande, Very Heavy Flavored Dibaryons, Phys. Rev. Lett. **124**, 212001 (2020).
[35] S. Gongyo, K. Sasaki, S. Aoki, T. Doi, T. Hatsuda, Y. Ikeda, T. Inoue, T. Iritani, N. Ishii, T. Miyamoto, and H. Nemura (HAL QCD Collaboration), Most Strange Dibaryon from Lattice QCD, Phys. Rev. Lett. **120**, 212001 (2018).
[36] S. Beane, W. Detmold, K. Orginos, and M. Savage, Nuclear physics from lattice QCD, Prog. Part. Nucl. Phys. **66**, 1 (2011).
[37] S. R. Beane, P. F. Bedaque, A. Parreno, and M. J. Savage, Two nucleons on a lattice, Phys. Lett. B **585**, 106 (2004).
[38] S. R. Beane, E. Chang, W. Detmold, H. W. Lin, T. C. Luu, K. Orginos, A. Parreno, M. J. Savage, A. Torok, and A. Walker-Loud (NPLQCD Collaboration), The deuteron and exotic two-body bound states from lattice QCD, Phys. Rev. D **85**, 054511 (2012).
[39] S. R. Beane, E. Chang, S. D. Cohen, W. Detmold, H.-W. Lin, T. C. Luu, K. Orginos, A. Parreño, M. J. Savage, and A. Walker-Loud (NPLQCD Collaboration), Hyperon-Nucleon Interactions from Quantum Chromodynamics and the Composition of Dense Nuclear Matter, Phys. Rev. Lett. **109**, 172001 (2012).
[40] T. Gershon and A. Poluektov, Displaced B_c^- mesons as an inclusive signature of weakly decaying double beauty hadrons, J. High Energy Phys. 01 (2019) 019.
[41] L. Ng, L. Bibrzycki, J. Nys, C. Fernandez-Ramirez, A. Pilloni, V. Mathieu, A. J. Rasmusson, and A. P. Szczepaniak (JPAC Collaboration), Deep learning exotic hadrons, Phys. Rev. D **105**, L091501 (2022).
[42] M. Albaladejo *et al.* (JPAC Collaboration), Novel approaches in hadron spectroscopy, Prog. Part. Nucl. Phys. **127**, 103981 (2022).
[43] J. Liu, Z. Zhang, J. Hu, and Q. Wang, Study of exotic hadrons with machine learning, Phys. Rev. D **105**, 076013 (2022).
[44] N. Mathur, M. Padmanath, and S. Mondal, Precise Predictions of Charmed-Bottom Hadrons from Lattice QCD, Phys. Rev. Lett. **121**, 202002 (2018).
[45] A. Bazavov, C. Bernard, J. Komijani, C. DeTar, L. Levkova, W. Freeman, S. Gottlieb, R. Zhou, U. M. Heller, J. E. Hetrick, J. Laiho, J. Osborn, R. L. Sugar, D. Toussaint, and R. S. Van de Water (MILC Collaboration), Lattice QCD ensembles with four flavors of highly improved staggered quarks, Phys. Rev. D **87**, 054505 (2013).

[46] E. Follana, Q. Mason, C. Davies, K. Hornbostel, G. P. Lepage, J. Shigemitsu, H. Trottier, and K. Wong (HPQCD and UKQCD Collaborations), Highly improved staggered quarks on the lattice, with applications to charm physics, Phys. Rev. D **75**, 054502 (2007).

[47] A. Bazavov, C. Bernard, N. Brown, J. Komijani, C. DeTar, J. Foley, L. Levkova, S. Gottlieb, U. M. Heller, J. Laiho, R. L. Sugar, D. Toussaint, and R. S. Van de Water (MILC Collaboration), Gradient flow and scale setting on MILC HISQ ensembles, Phys. Rev. D **93**, 094510 (2016).

[48] G. P. Lepage, L. Magnea, C. Nakhleh, U. Magnea, and K. Hornbostel, Improved nonrelativistic QCD for heavy quark physics, Phys. Rev. D **46**, 4052 (1992).

[49] R. J. Dowdall, B. Colquhoun, J. O. Daldrop, C. T. H. Davies, I. D. Kendall, E. Follana, T. C. Hammant, R. R. Horgan, G. P. Lepage, C. J. Monahan, and E. H. Müller (HPQCD Collaboration), The upsilon spectrum and the determination of the lattice spacing from lattice QCD including charm quarks in the sea, Phys. Rev. D **85**, 054509 (2012).

[50] A. X. El-Khadra, A. S. Kronfeld, and P. B. Mackenzie, Massive fermions in lattice gauge theory, Phys. Rev. D **55**, 3933 (1997).

[51] M. Tanabashi *et al.* (Particle Data Group), Review of particle physics, Phys. Rev. D **98**, 030001 (2018).

[52] S. Basak, R. Edwards, G. T. Fleming, U. M. Heller, C. Morningstar, D. Richards, I. Sato, and S. J. Wallace (Lattice Hadron Physics (LHPC) Collaboration), Clebsch-Gordan construction of lattice interpolating fields for excited baryons, Phys. Rev. D **72**, 074501 (2005).

[53] See Supplemental Material at http://link.aps.org/supplemental/10.1103/PhysRevLett.130.111901 for results on other lattices, fit details, and error budget, which includes Refs. [54–63].

[54] R. G. Edwards, J. J. Dudek, D. G. Richards, and S. J. Wallace, Excited state baryon spectroscopy from lattice QCD, Phys. Rev. D **84**, 074508 (2011).

[55] R. G. Edwards, N. Mathur, D. G. Richards, and S. J. Wallace (Hadron Spectrum Collaboration), Flavor structure of the excited baryon spectra from lattice QCD, Phys. Rev. D **87**, 054506 (2013).

[56] M. Padmanath, R. G. Edwards, N. Mathur, and M. Peardon, Spectroscopy of triply-charmed baryons from lattice QCD, Phys. Rev. D **90**, 074504 (2014).

[57] S. Meinel, Excited-state spectroscopy of triply-bottom baryons from lattice QCD, Phys. Rev. D **85**, 114510 (2012).

[58] S. R. Beane, W. Detmold, T. C. Luu, K. Orginos, A. Parreno, M. J. Savage, A. Torok, and A. Walker-Loud, High Statistics analysis using anisotropic clover lattices: (I) Single hadron correlation functions, Phys. Rev. D **79**, 114502 (2009).

[59] H.-W. Lin and S. D. Cohen, Lattice QCD beyond ground states, in *Proceedings of the 4th International Workshop on Numerical Analysis and Lattice QCD* (2007), arXiv:0709.1902.

[60] S. Borsanyi *et al.*, *Ab initio* calculation of the neutron-proton mass difference, Science **347**, 1452 (2015).

[61] C. McNeile, C. T. H. Davies, E. Follana, K. Hornbostel, and G. P. Lepage, Heavy meson masses and decay constants from relativistic heavy quarks in full lattice QCD, Phys. Rev. D **86**, 074503 (2012).

[62] R. J. Dowdall, C. T. H. Davies, T. C. Hammant, and R. R. Horgan, Precise heavy-light meson masses and hyperfine splittings from lattice QCD including charm quarks in the sea, Phys. Rev. D **86**, 094510 (2012).

[63] B. Chakraborty, C. T. H. Davies, B. Galloway, P. Knecht, J. Koponen, G. C. Donald, R. J. Dowdall, G. P. Lepage, and C. McNeile, High-precision quark masses and QCD coupling from $n_f = 4$ lattice QCD, Phys. Rev. D **91**, 054508 (2015).

[64] C. T. H. Davies, K. Hornbostel, A. Langnau, G. P. Lepage, A. Lidsey, J. Shigemitsu, and J. H. Sloan, Precision Υ spectroscopy from nonrelativistic lattice QCD, Phys. Rev. D **50**, 6963 (1994).

[65] M. Wurtz, R. Lewis, and R. M. Woloshyn, Free-form smearing for bottomonium and B meson spectroscopy, Phys. Rev. D **92**, 054504 (2015).

[66] R. J. Hudspith, B. Colquhoun, A. Francis, R. Lewis, and K. Maltman, A lattice investigation of exotic tetraquark channels, Phys. Rev. D **102**, 114506 (2020).

[67] B. G. R. de Prony, Essai experimental et analytique: Sur les lois de la dilatabilit e de fluides elastique et sur celles de la force expansive de la vapeur de l'alkool, a diff erentes temp eratures, J. Ec. Polytech. **1(22)**, 24 (1975).

[68] G. T. Fleming, What can lattice QCD theorists learn from NMR spectroscopists?, in *Proceedings of the 3rd International Workshop on Numerical Analysis and Lattice QCD* (2004), pp. 143–152, arXiv:hep-lat/0403023.

[69] S. Kunis, T. Peter, T. Roemer, and U. von der Ohe, A multivariate generalization of Prony's method, arXiv:1506.00450.

[70] M. Padmanath and S. Prelovsek, Signature of a Doubly Charm Tetraquark Pole in DD* Scattering on the Lattice, Phys. Rev. Lett. **129**, 032002 (2022).

[71] P. Zyla *et al.* (Particle Data Group), Review of particle physics, Prog. Theor. Exp. Phys. **2020**, 083C01 (2020).

[72] Z. S. Brown, W. Detmold, S. Meinel, and K. Orginos, Charmed bottom baryon spectroscopy from lattice QCD, Phys. Rev. D **90**, 094507 (2014).

[73] M. Karliner and J. L. Rosner, Discovery of Doubly-Charmed Ξ_{cc} Baryon Implies a Stable ($bb\bar{u}\,\bar{d}$) Tetraquark, Phys. Rev. Lett. **119**, 202001 (2017).

[74] E. J. Eichten and C. Quigg, Heavy-Quark Symmetry Implies Stable Heavy Tetraquark Mesons $Q_iQ_j\bar{q}_k\bar{q}_l$, Phys. Rev. Lett. **119**, 202002 (2017).

[75] R. Aaij *et al.* (LHCb Collaboration), Observation of an exotic narrow doubly charmed tetraquark, Nat. Phys. **18**, 751 (2022).

[76] R. Aaij *et al.* (LHCb Collaboration), Observation of a Narrow Pentaquark State, $P_c(4312)^+$, and of Two-Peak Structure of the $P_c(4450)^+$, Phys. Rev. Lett. **122**, 222001 (2019).

[77] R. Aaij *et al.* (LHCb Collaboration), Observation of structure in the J/ψ-pair mass spectrum, Sci. bull. **65**, 1983 (2020).

[78] C. Morningstar, J. Bulava, B. Singha, R. Brett, J. Fallica, A. Hanlon, and B. Hörz, Estimating the two-particle K-matrix for multiple partial waves and decay channels from finite-volume energies, Nucl. Phys. **B924**, 477 (2017).